

Low-energy phonons and superconductivity in $\text{Sn}_{0.8}\text{In}_{0.2}\text{Te}$

Zhijun Xu,^{1,2,3} J. A. Schneeloch,^{1,4} Ruidan Zhong,^{1,5} J. A. Rodriguez-Rivera,^{6,7}
L. Harriger,⁶ R. J. Birgeneau,^{2,3} Genda Gu,¹ J. M. Tranquada,¹ and Guangyong Xu¹

¹Condensed Matter Physics and Materials Science Department,
Brookhaven National Laboratory, Upton, New York 11973, USA

²Physics Department, University of California, Berkeley, California 94720, USA

³Materials Science Division, Lawrence Berkeley National Laboratory, Berkeley, California 94720, USA

⁴Department of Physics, Stony Brook University, Stony Brook, New York 11794, USA

⁵Materials Science and Engineering Department, Stony Brook University, Stony Brook, New York 11794, USA

⁶NIST Center for Neutron Research, National Institute of Standards and Technology, Gaithersburg, Maryland 20899, USA

⁷Department of Materials Science & Engineering, University of Maryland, College Park, MD 20742, USA

(Dated: June 20, 2021)

We present neutron scattering measurements on low-energy phonons from a superconducting ($T_c = 2.7$ K) $\text{Sn}_{0.8}\text{In}_{0.2}\text{Te}$ single crystal sample. The longitudinal acoustic phonon mode and one transverse acoustic branch have been mapped out around the (002) Bragg peak for temperatures of 1.7 K and 4.2 K. We observe a substantial energy width of the transverse phonons at energies comparable to twice the superconducting gap; however, there is no change in this width between the superconducting and normal states. We also confirm that the compound is well ordered, with no indications of structural instability.

PACS numbers: 74.70.-b, 74.25.Kc, 78.70.Nx

I. INTRODUCTION

The discovery of the topological insulators (TIs),^{1,2} which are insulating (theoretically) in the bulk but have metallic surface states present due to their topologically nontrivial electronic structure, have attracted great scientific interest. These materials can be categorized by the symmetry by which their surface states are protected. For example, the "topological crystalline insulators" (TCIs)^{3,4} have surface states protected by certain crystal point group symmetries rather than by time-reversal symmetry invariance (TRI-TIs),^{1,5} as observed in other compounds.

The studies of TRI-TIs and TCIs have stimulated the search for an even more exotic state of matter, the topological superconductor (TS), whose surface states are predicted to be Majorana fermions.^{6,7} One candidate is $\text{Cu}_x\text{Bi}_2\text{Se}_3$, a superconductor arising from Cu-doping of the TRI-TI Bi_2Se_3 .⁸ The most important evidence for (or against) the existence of TS in particular compounds has come from the presence (or absence) of a zero-bias conductance peak (ZBCP) in point-contact spectra. Such a peak may be indicative of unconventional superconductivity, and calculations have shown that every possible unconventional pairing symmetry for $\text{Cu}_x\text{Bi}_2\text{Se}_3$ should be topologically nontrivial^{9,10}. Some groups have reported such a peak in $\text{Cu}_x\text{Bi}_2\text{Se}_3$ ¹⁰⁻¹², though other groups have raised doubts on these measurements^{13,14}. Furthermore, the diamagnetic shielding fraction in $\text{Cu}_x\text{Bi}_2\text{Se}_3$ varies significantly and is usually very low⁸, limiting possible studies.

Another system of interest is based on SnTe . Pure SnTe has been proposed¹⁵ and demonstrated⁴ to be a topological crystalline insulator; furthermore, it has a ferroelectric phase at low temperature^{16,17} and intriguing thermoelectric properties at high temperature.¹⁸ More relevant to the present study is that $\text{Sn}_{1-\delta}\text{Te}$ is superconducting at temperature well below 1 K.¹⁹ Substitution of a small amount of In for Sn drives the ferroelectric instability to zero, while increasing the su-

perconducting T_c .²⁰ More recent studies have shown that T_c grows linearly with In concentration, reaching ~ 4.5 K for $\text{Sn}_{0.55}\text{In}_{0.45}\text{Te}$.^{21,22}

The superconductivity in $\text{Sn}_{1-\delta}\text{Te}$ was originally explained by electron-phonon coupling involving the scattering of carriers between equivalent conduction band-valleys.^{19,23} It has been noted more recently that the hybridization between valence and conduction bands that leads to band inversion and topological effects also leads to enhanced van Hove singularities, and that this increased density of states might be helpful to superconductivity.²⁴ When T_c was raised by substitution of In, Erickson *et al.*²⁰ considered the possibility of pairing enhancement via negative U centers associated with In. Sasaki *et al.*²⁵ observed a zero-bias conduction peak in a point-contact measurement on $\text{Sn}_{1-x}\text{In}_x\text{Te}$ with $x = 0.45$, arguing that this is evidence for an odd-parity superconducting state. In contrast, Saghir *et al.*²⁶ have measured the temperature dependence of the magnetic penetration depth by muon spin rotation spectroscopy and find that it is consistent with an s -wave gap. They also find evidence for strong coupling, which may be necessary given the large magnitude of the normal-state resistivity found in In-doped SnTe crystals.²² Clearly, resolving the character of the superconducting state in this system is of considerable current interest.

In this paper, we report low-energy neutron scattering measurements on a superconducting single-crystal of $\text{Sn}_{0.8}\text{In}_{0.2}\text{Te}$ with $T_c = 2.7$ K. Finding no evidence for any structural instability at low temperature, we have characterized longitudinal and transverse acoustic phonon dispersions in this sample below and above T_c . The phonon dispersion relations in the superconducting sample are consistent with these results in the parent compound SnTe .^{18,27} For a superconductor in which pairing is due to electron-phonon coupling, one expects to see characteristic changes in the phonon self energy for phonon energies comparable to 2Δ , where Δ is the energy of the superconducting gap.²⁸⁻³² We find instead a surprisingly large

energy width for phonon energy $\hbar\omega \sim 2\Delta$, with no significant change across T_c . We discuss possible causes of this large self energy.

II. EXPERIMENTAL DETAILS

The single-crystal sample used in this experiment was grown by a modified floating-zone method^{22,33} at Brookhaven National Laboratory. The mass is 22 g. The zero field cooled (ZFC) susceptibilities and resistivity, measured with a superconducting quantum interference device (SQUID) magnetometer, are shown in Fig. 1(a), suggesting a bulk $T_c \approx 2.7$ K. The samples have also been characterized by x-ray diffraction, indicating a rocksalt cubic structure.²²

Neutron scattering experiments were carried out on the triple-axis spectrometer SPINS and on the Multi-Axis Crystal Spectrometer (MACS)³⁴ located at the NIST Center for Neutron Research (NCNR). We used horizontal beam collimations of Guide-80'-S-80'-240' (S = sample) with a fixed final energy of 5 meV on SPINS together with a cooled Be filter after the sample to reduce higher-order neutrons. We used a fixed final energy of 5.1 meV, with BeO filters after the sample and a PG filter before the sample, and horizontal collimations of open-PG-open-S-90'-BeO-open on MACS.

The inelastic neutron scattering measurements have been performed in the (HHL) scattering plane. The lattice constants for this sample are $a = b = c \approx 6.33$ Å. The data are described in reciprocal lattice units (r.l.u.) of $(a^*, b^*, c^*) = (2\pi/a, 2\pi/b, 2\pi/c)$.

III. RESULTS AND DISCUSSIONS

The elastic scattering in the (HHL) plane from MACS at $T = 1.7$ K $< T_c$ is shown in Fig. 1(b). The relatively low intensity of the $(1,1,1)$ peak and the absence of Bragg peaks at $(1,1,0)$ or $(0,0,1)$ are consistent with the rocksalt cubic structure.²² There is no evidence of any superlattice or diffuse scattering that might indicate a structural instability. Hence, we focus our studies on the transverse (TA) and longitudinal (LA) acoustic phonons around the strong $(0,0,2)$ peak as shown in Fig. 1(b).

In Fig. 2 (a)-(b), we plot constant- Q scans from data taken at SPINS at various wave vectors along the transverse direction to show the TA_1 phonon mode (polarized along $[001]$ and propagating along $[110]$). The phonon peaks are fitted with Lorentzian functions, plus a Gaussian function describing the elastic peak. The fitted curves are plotted with the data. We can see that the TA phonons are all well defined. The energy center, energy width, and intensity of the phonon modes can be obtained in the fitting. The phonon dispersion relations are plotted in fig. 2 (c)-(d). The phonon dispersion relations measured at both 1.7 K and 4.2 K are overall consistent with previous inelastic neutron scattering measurements on the parent compound SnTe.^{18,27} Those studies reported that the band top for the $[110]$ acoustic phonon is around 5 meV, which is the same as in our results.

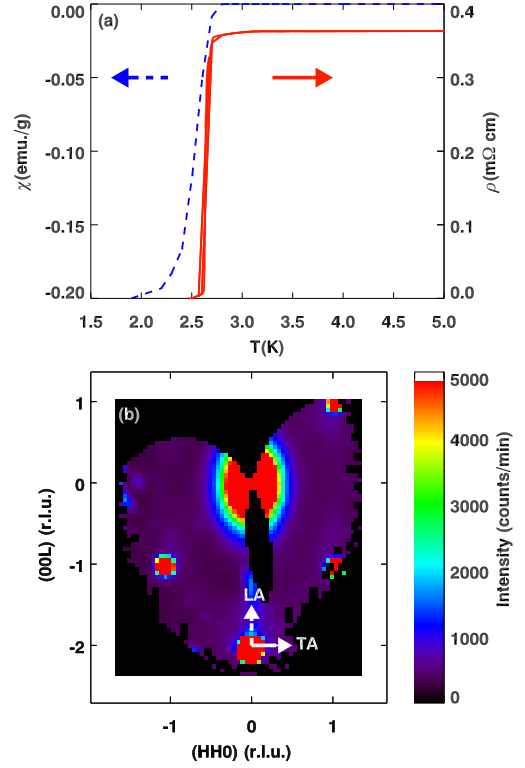


FIG. 1: (Color online) (a) Temperature dependence of ZFC magnetization (blue dash line, left side) and resistivity (red solid line, right side, from Ref. 22). (b) Elastic scans in scattering plane (HHL) at 1.7 K. The dashed and solid arrows show the longitudinal acoustic phonon (LA) and transverse acoustic phonon (TA) measured around Bragg peak (002) , respectively.

Mesh scans (constant energy measurements from MACS) were also performed around the (002) Bragg peak to map out the phonon modes along both the transverse and longitudinal directions. We plot intensity maps in energy-momentum space in Fig. 3. The white lines shown here are guides to the eye that describe the phonon dispersions. The dispersion relations of both the TA and LA modes are in good agreement with previously reported data as well as recent neutron scattering measurements on the parent compound SnTe,^{18,27} suggesting that a 20% In doping does not significantly modify the low-energy lattice dynamics in this material.

In the parent SnTe and a similar compound PbTe, a soft transverse optic (TO) mode has been observed, that condenses into a column type intensity near zone-center at low temperatures.^{16,18,27,35–37} Limited by the energy and Q range of our measurements, we are not able to map out the entire band for this TO mode. Nevertheless, we did look for the column type intensity in our SPINS measurements (Fig. 1), but have not noticed any additional intensity, beyond the transverse acoustic phonons, that could suggest a soft TO mode. This mode, associated with the ferroelectric instability, is screened by free carriers^{19,27}, so that it is possible that the large In concentration in our sample has stiffened the TO mode sufficiently that it is not present in our energy window. It is also possible that we have not detected it due to a smaller TO phonon structure

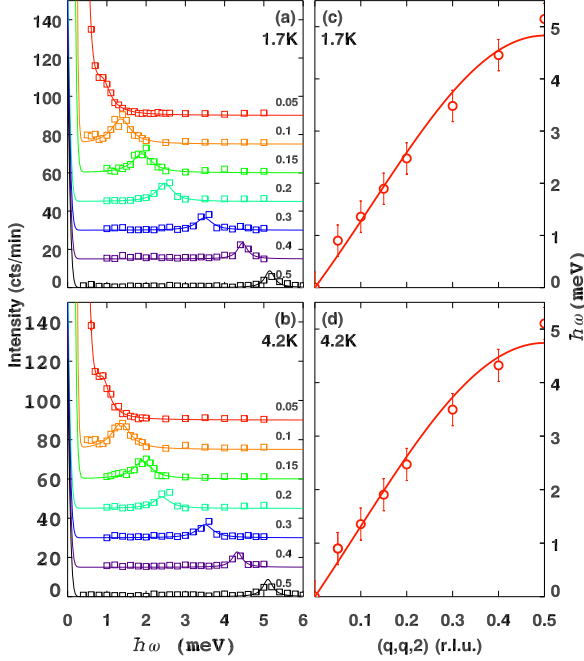


FIG. 2: (Color online) (a,b) Constant- q cuts of phonon spectra along transverse directions near (002) Bragg peak at (a) 1.7 K and (b) 4.2 K and at various \mathbf{Q} positions with $\mathbf{Q} = (q, q, 2)$, with $q = 0.05$ (red), 0.1 (orange), 0.15 (green), 0.2 (teal), 0.3 (blue), 0.4 (purple), and 0.5 (black). The data are taken on SPINS. (c,d) The TA_1 phonon dispersions around (002) at (c) 1.7 K and (d) 4.2 K. The phonon energies are obtained from fitting the energy cuts from (a)-(b) as described in the text. The lines are guides to the eye. The errors are obtained from the fitting process.

factor, compared to that of the acoustic phonon, near (002).

We now look at all the parameters obtained from the fits to the data. The dynamic response $\chi''(\mathbf{Q}, \hbar\omega) = (1 - e^{-\hbar\omega/k_B T})S(\mathbf{Q}, \hbar\omega)$ is the measured neutron scattering intensity divided by the Bose factor. Here the natural temperature dependence of the phonon intensities has been taken out so that we can look at any intrinsic changes directly. The products $\hbar\omega\chi(Q, \omega)$ at different temperatures ($T = 1.7$ and 4.2 K) are shown in the upper panels of Fig. 4. This product remains almost constant for all q values for the TA mode at both temperatures, suggesting a highly harmonic mode. For the LA phonon mode, we see one high point for $q = 0.07$, while the product remains almost constant for all other q values. This high point at small q could be a possible result of the anomalously broad soft TO phonon mode near zone center^{18,37} observed in PbTe and SnTe at low temperatures. The measured phonon energies and momentum widths are shown in the lower panels of Fig. 4. The energy widths, 2Γ , which are inversely proportional to the phonon lifetime, are obtained from the constant- Q scans from SPINS shown in Fig. 2. The q -widths, shown in Fig. 4 (d), are extracted from the LA phonon measured on MACS.

Based on previous studies of the change in phonon self en-

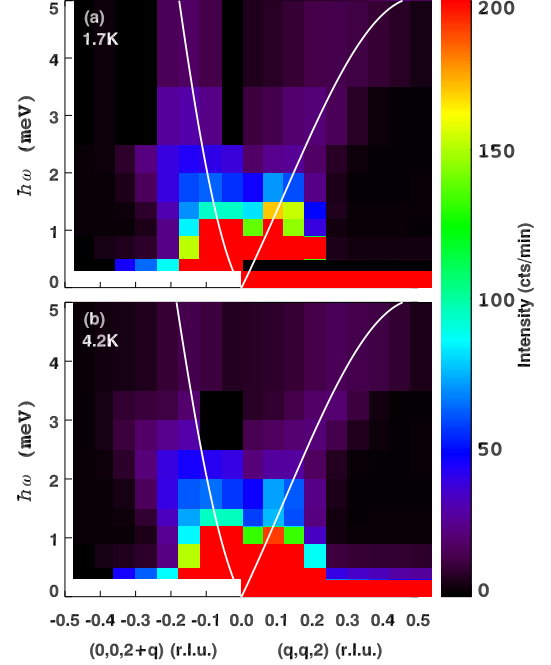


FIG. 3: (Color online) Phonon intensity plots in energy-momentum space around Bragg peak (002) at (a) 1.7 K and (b) 4.2 K. For each panel, the left half corresponds to longitudinal phonons going along [001] direction; and the right half corresponds to transverse phonons going along the [110] direction. The white lines are phonon dispersions obtained from fitting of the energy cuts.

ergy due to superconducting order,^{28,29,38} we expect to see the largest effects near the energy 2Δ , where Δ is the superconducting gap. On cooling below T_c , one expects to see an increase in the line width for $\hbar\omega \gtrsim 2\Delta$ and a decrease for $\hbar\omega \lesssim 2\Delta$. The recent work of Saghir *et al.*²⁶ indicates strong coupling, with $2\Delta \approx 4k_B T_c$, which yields an estimate of $2\Delta \sim 0.9$ meV for our crystal with $T_c = 2.7$ K. This is roughly consistent with a point-contact measurement on a sample of $\text{Sn}_{1-x}\text{In}_x\text{Te}$ with $x = 0.045$ $T_c = 1.2$ K which observed $2\Delta \sim 0.2$ meV.²⁵ The lowest phonon energy we can measure is limited by the instrumental resolution ($\delta E \sim 0.35$ meV for SPINS, $\delta E \sim 0.5$ meV for MACS at $\hbar\omega=0$ meV) is around $\hbar\omega \lesssim 1$ meV, close to the estimated value of 2Δ .

The effective energy resolution for the TA mode depends on how the anisotropic resolution function matches up with the dispersion; this is the focusing effect, which is discussed in Ref. 28. For most of the wave vectors covered, the velocity is relatively constant, and we calculate an effective energy width of ~ 0.15 meV, taking into account the sample mosaic. This is quite close to the measured widths for $H = 0.3$ and 0.4, shown in Fig. 4(c), so those measurements appear to be resolution limited. The effective resolution width at the zone boundary rises because of flattening of the dispersion. In contrast, the measured width near $H = 0.1$ becomes much larger than the effective resolution. The phonon energy in this region is close to 2Δ ; however, we see no significant change

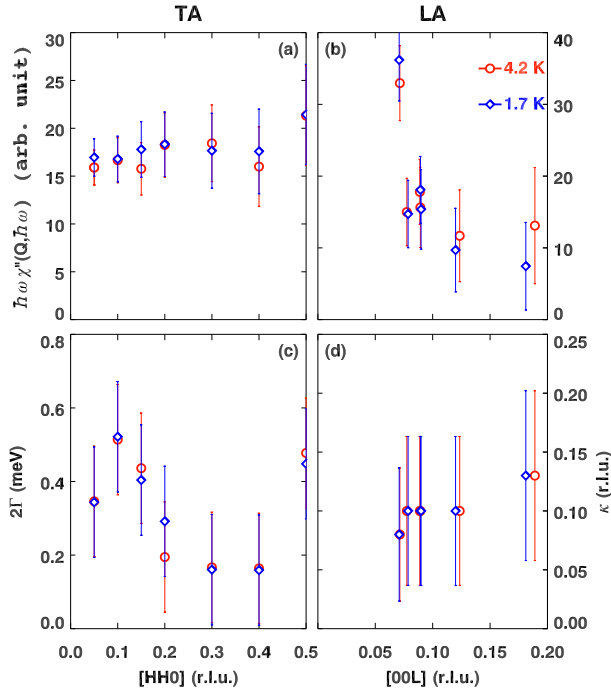


FIG. 4: (Color online) Summary of the fitting parameters. (a,b) The dynamic response χ'' multiplied by phonon energy $\hbar\omega$ for acoustic phonons measured along (a) transverse [110] direction, and (b) longitudinal [001] directions at various q positions. (c) The energy width 2Γ for the TA₁ phonon mode measured on SPINS. (d) The q width for the LA phonon measured on MACS. In (a)-(b), the errors represent ± 1 standard deviation. In (c)-(d), the errors are obtained from the fitting process.

in the energy width between the superconducting and normal states. While the width changes due to superconducting order are expected to be small,²⁸ the large, temperature-independent contribution certainly makes their detection more challenging.

What could be the cause of this large energy width at small q ? One possibility is that is due to interactions with the soft TO mode. Another possibility is that these low- q phonons are involved in scattering electrons within a small pocket at the Fermi surface. According to Allen and Cohen,¹⁹ such interactions contribute little to electron pairing; the main contribution comes from scattering between different pockets, which involves phonons at large q . Further experimental work would be necessary to identify such an effect in the phonon widths.

IV. SUMMARY

Overall, we have performed low energy neutron scattering measurements on a single crystal of Sn_{0.8}In_{0.2}Te. There is no evidence of structural instability in this sample. Two acoustic phonon modes (TA₁ along [110] and LA along [001]) have been mapped out at temperatures below and above T_c . The acoustic phonon dispersion relations are consistent with those in the parent topological insulator SnTe. A large, temperature-independent phonon energy width at $\hbar\omega \sim 2\Delta$ obscures any change associated with the onset of superconductivity, but indicates that strong interactions may be present.

Acknowledgments

J.A.S. and R.Z. are supported by the Center for Emergent Superconductivity, an Energy Frontier Research Consortium supported by the Office of Basic Energy Science of the Department of Energy. The work at Brookhaven National Laboratory and Lawrence Berkeley National Laboratory was supported by the Office of Basic Energy Sciences (BES), Division of Materials Science and Engineering, U.S. Department of Energy (DOE), under Contract Nos. DE-AC02-98CH10886 and DE-AC02-05CH1123, respectively. This work utilized facilities supported in part by the National Science Foundation under Agreement No. DMR-0944772.

- ¹ L. Fu, C. L. Kane, and E. J. Mele, Phys. Rev. Lett. **98**, 106803 (2007).
- ² M. Z. Hasan and C. L. Kane, Rev. Mod. Phys. **82**, 3045 (2010).
- ³ L. Fu, Phys. Rev. Lett. **106**, 106802 (2011).
- ⁴ Y. Tanaka, Z. Ren, T. Sato, K. Nakayama, S. Souma, T. Takahashi, K. Segawa, and Y. Ando, Nat. Phys. **8**, 800 (2012).
- ⁵ Y. Xia, D. Qian, D. Hsieh, L. Wray, A. Pal, H. Lin, A. Bansil, D. Grauer, Y. S. Hor, R. J. Cava, et al., Nat. Phys. **5**, 398 (2009).
- ⁶ L. Fu and C. L. Kane, Phys. Rev. Lett. **100**, 096407 (2008).
- ⁷ X.-L. Qi and S.-C. Zhang, Rev. Mod. Phys. **83**, 1057 (2011).
- ⁸ Y. S. Hor, A. J. Williams, J. G. Checkelsky, P. Roushan, J. Seo, Q. Xu, H. W. Zandbergen, A. Yazdani, N. P. Ong, and R. J. Cava, Phys. Rev. Lett. **104**, 057001 (2010).
- ⁹ L. Fu and E. Berg, Phys. Rev. Lett. **105**, 097001 (2010).
- ¹⁰ S. Sasaki, M. Kriener, K. Segawa, K. Yada, Y. Tanaka, M. Sato, and Y. Ando, Phys. Rev. Lett. **107**, 217001 (2011).
- ¹¹ T. Kirzhner, E. Lahoud, K. B. Chaska, Z. Salman, and A. Kanigel, Phys. Rev. B **86**, 064517 (2012).

- ¹² X. Chen, C. Huan, Y. S. Hor, C. A. R. Sá de Melo, and Z. Jiang, arXiv:1210.6054 (2012).
- ¹³ N. Levy, T. Zhang, J. Ha, F. Sharifi, A. A. Talin, Y. Kuk, and J. A. Stroscio, Phys. Rev. Lett. **110**, 117001 (2013).
- ¹⁴ H. Peng, D. De, B. Lv, F. Wei, and C.-W. Chu, Phys. Rev. B **88**, 024515 (2013).
- ¹⁵ T. H. Hsieh, H. Lin, J. Liu, W. Duan, A. Bansil, and L. Fu, Nat. Commun. **3**, 982 (2012).
- ¹⁶ G. S. Pawley, W. Cochran, R. A. Cowley, and G. Dolling, Phys. Rev. Lett. **17**, 753 (1966).
- ¹⁷ K. L. I. Kobayashi, Y. Kato, Y. Katayama, and K. F. Komatsubara, Phys. Rev. Lett. **37**, 772 (1976).
- ¹⁸ C. W. Li, O. Hellman, J. Ma, A. F. May, H. B. Cao, X. Chen, A. D. Christianson, G. Ehlers, D. J. Singh, B. C. Sales, et al., Phys. Rev. Lett. **112**, 175501 (2014).
- ¹⁹ P. B. Allen and M. L. Cohen, Phys. Rev. **177**, 704 (1969).
- ²⁰ A. S. Erickson, J. H. Chu, M. F. Toney, T. H. Geballe, and I. R. Fisher, Phys. Rev. B **79**, 024520 (2009).

- ²¹ G. Balakrishnan, L. Bawden, S. Cavendish, and M. R. Lees, Phys. Rev. B **87**, 140507 (2013).
- ²² R. D. Zhong, J. A. Schneeloch, X. Y. Shi, Z. J. Xu, C. Zhang, J. M. Tranquada, Q. Li, and G. D. Gu, Phys. Rev. B **88**, 020505 (2013).
- ²³ M. L. Cohen, Phys. Rev. **134**, A511 (1964).
- ²⁴ X.-G. He, X. Xi, and W. Ku, *Generic Symmetry Breaking Instability of Topological Insulators due to a Novel van Hove Singularity*, arXiv:1410.2885 ((2014)).
- ²⁵ S. Sasaki, Z. Ren, A. A. Taskin, K. Segawa, L. Fu, and Y. Ando, Phys. Rev. Lett. **109**, 217004 (2012).
- ²⁶ M. Saghir, J. A. T. Barker, G. Balakrishnan, A. D. Hillier, and M. R. Lees, Phys. Rev. B **90**, 064508 (2014).
- ²⁷ E. R. Cowley, J. K. Darby, and G. S. Pawley, J. Phys. C: Solid State Phys. **2**, 1916 (1969).
- ²⁸ S. M. Shapiro, G. Shirane, and J. D. Axe, Phys. Rev. B **12**, 4899 (1975).
- ²⁹ P. B. Allen, V. N. Kostur, N. Takesue, and G. Shirane, Phys. Rev. B **56**, 5552 (1997).
- ³⁰ F. Weber, A. Kreyssig, L. Pintschovius, R. Heid, W. Reichardt, D. Reznik, O. Stockert, and K. Hradil, Phys. Rev. Lett. **101**, 237002 (2008).
- ³¹ P. B. Allen, Solid State Commun. **14**, 937 (1974).
- ³² P. B. Allen, B. Mitrović, F. S. Henry Ehrenreich, and T. David, in *Solid State Physics* (Academic Press, 1983), vol. 37, pp. 1–92.
- ³³ R. D. Zhong, J. A. Schneeloch, T. S. Liu, F. E. Camino, J. M. Tranquada, and G. D. Gu, Phys. Rev. B **90**, 020505 (2014).
- ³⁴ J. A. Rodriguez, D. M. Adler, P. C. Brand, C. Broholm, J. C. Cook, C. Brocker, R. Hammond, Z. Huang, P. Hundertmark, J. W. Lynn, et al., Meas. Sci. Technol. **19**, 034023 (2008).
- ³⁵ E. S. Božin, C. D. Malliakas, P. Souvatzis, T. Proffen, N. A. Spaldin, M. G. Kanatzidis, and S. J. L. Billinge, Science **330**, 1660 (2010).
- ³⁶ K. R. Knox, E. S. Božin, C. D. Malliakas, M. G. Kanatzidis, and S. J. L. Billinge, Phys. Rev. B **89**, 014102 (2014).
- ³⁷ J. Ma, O. Delaire, E. D. Specht, A. F. May, O. Gourdon, J. D. Budai, M. A. McGuire, T. Hong, D. L. Abernathy, G. Ehlers, et al., Phys. Rev. B **90**, 134303 (2014).
- ³⁸ J. D. Axe and G. Shirane, Phys. Rev. Lett. **30**, 214 (1973).